Karabük Üniversitesi
DÇE Doğa Bilimleri Dergisi

(NSJ-ISI)

e-ISSN: 2757 8224
Cilt 6, Sayı 2
Aralık 2025, 61-76
Araştırma Makalesi

University of Karabuk
ISI Natural Sciences Journal

(NSJ-ISI)

e-ISSN: 2757 8224
Volume 6, Issue 2
December 2025, 61-76
Research Article

Investigation of Gas Nitrided 42CrMo4 and 34CrNiAl7 Steels for Gear and Shaft Applications

Volkan Karakurt [1*], Orçun Zığındere[1], Talip Çıtrak[1], Feyzanur Öztürk[1]

[1]*Sağlam Metal San. ve Tic. A.Ş., /Kocaeli, TÜRKİYE*

***Başvuru/Received**: 10/06/2025* ***Kabul / Accepted**: 19/08/2025* ***Çevrimiçi Basım / Published Online:** 31/12/2025*

***Son Versiyon/Final Version**: 19/08/2025*

Abstract

In this study, the microstructure, surface hardness, and wear behavior of 42CrMo4 and 34CrNiAl7 steels—commonly used in continuously operating components such as gears and shafts—were compared following gas nitriding treatment. Initially, the samples underwent quenching and tempering heat treatments, after which gas nitriding was applied under identical conditions. Microstructural characterization, surface hardness measurements, and effective case depth analyses were conducted on the nitrided samples. Furthermore, the wear behavior of the nitrided surfaces was evaluated through reciprocating dry sliding wear tests using an Al_2O_3 ceramic ball under applied loads of 10 N and 15 N over a sliding distance of 1000 meters. Post-nitriding results revealed that the surface hardness of 42CrMo4 and 34CrNiAl7 steels increased by 169% and 339%, respectively. Microstructural observations revealed that the white layer on the surface of 42CrMo4 was 4.78 µm thicker than that on 34CrNiAl7. Wear test results demonstrated that 42CrMo4 exhibited 40% greater wear loss than 34CrNiAl7 under a 10 N load, and 56% greater wear loss under a 15 N load. The superior wear resistance of 34CrNiAl7 is attributed to the formation of a harder nitrided surface layer. From an industrial standpoint, the selection of nitrided steel should be guided by the severity of wear conditions. For components subjected to high mechanical stress and severe wear-such as aerospace landing gear, high-load gears, and metal forming tools-gas-nitrided 34CrNiAl7 steel is recommended due to its superior surface hardness and wear resistance. Conversely, for applications involving moderate wear, such as hydraulic rods, camshafts, and general-purpose industrial shafts, gas-nitrided 42CrMo4 steel offers a cost-effective and sufficiently durable alternative, balancing toughness and wear resistance.

Keywords: Material Selection, 34CrNiAl7 (DIN 1.8550), 42CrMo4 (AISI 4140), Gas Nitriding, Wear Resistance, Friction Coefficient.

Özet

Bu çalışmada, dişliler ve miller gibi sürekli çalışan bileşenlerde yaygın olarak kullanılan 42CrMo4 ve 34CrNiAl7 çeliklerinin gaz nitrürleme işlemi sonrası mikroyapısı, yüzey sertliği ve aşınma davranışı karşılaştırılmıştır. Numunelere öncelikle yağda su verme ve temperleme ısıl işlemi, ardından aynı koşullar altında gaz nitrürleme uygulanmıştır. Numunelerde mikroyapı karakterizasyonu, yüzey sertliği ölçümleri ve etkin sertlik derinliği analizleri gerçekleştirilmiştir. Ayrıca, nitrürlenmiş yüzeylerin aşınma davranışı, 1000 metre kayma mesafesinde 10 N ve 15 N yükler altında Al_2O_3 seramik bilye kullanılarak ileri geri kuru kayma aşınma deneyleri ile değerlendirilmiştir. Nitrürleme sonrası sonuçlar, 42CrMo4 ve 34CrNiAl7 çeliklerinin yüzey sertliğinin sırasıyla %169 ve %339 oranında arttığını göstermiştir. Mikroyapısal gözlemlerde, 42CrMo4 yüzeyinde oluşan beyaz tabakanın 34CrNiAl7'den 4,78 µm daha kalın olduğu belirlenmiştir. Aşınma testi sonuçları, 42CrMo4'ün 10 N yük altında 34CrNiAl7'den %40, 15 N yük altında ise %56 daha fazla aşınma kaybı sergilediğini göstermiştir. 34CrNiAl7'nin üstün aşınma direnci, daha sert bir nitrürlenmiş yüzey tabakasının oluşumuna atfedilmiştir. Endüstriyel bakış açısından değerlendirildiğinde, nitrürlenmiş çelik seçimi aşınma koşullarının şiddetine göre yapılmalıdır. Havacılık iniş takımları, yüksek yüklü takımlar ve metal şekillendirme araçları gibi yüksek mekanik gerilime ve şiddetli aşınmaya maruz kalan bileşenler için, üstün yüzey sertliği ve aşınma direnci

nedeniyle gaz nitrürlenmiş 34CrNiAl7 çeliği önerilir. Buna karşılık, hidrolik çubuklar, eksantrik milleri ve genel amaçlı endüstriyel miller gibi orta düzeyde aşınma içeren uygulamalar için gaz nitrürlemeli 42CrMo4 çeliği, tokluk ve aşınma direncini dengeleyen uygun maliyetli ve yeterince dayanıklı bir alternatif sunar.

Anahtar Kelimeler: Malzeme Seçimi, DIN 1.8550 (34CrNiAl7), AISI 4140 (42CrMo4), Gaz Nitrürleme, Aşınma Direnci, Sürtünme Katsayısı.

1.Introduction

Steels are iron-carbon alloys containing carbon in the range of 0.02–2.06% [1]. These materials are classified according to their application, chemical composition, manufacturing processes, and heat treatment techniques. Machine manufacturing steels constitute a category of steels tailored for specific mechanical applications. They are primarily employed in the production of machine components, including shafts, gears, and various fasteners such as bolts, nuts, rivets, and studs [2].

Gears and shafts are essential components in mechanical systems and are frequently exposed to wear due to continuous loading, friction, and relative motion. The wear-related damage observed on the surfaces of gears and shafts is illustrated in Figure 1. As these components wear, their dimensional accuracy deteriorates, leading to increased vibration, noise, and energy loss, ultimately compromising overall machine performance. Furthermore, worn gear teeth may fail to mesh properly, potentially resulting in complete system failure [3–4]. Therefore, the wear resistance of steels used in gears, mills, and shafts must be carefully evaluated. The use of materials with poor wear resistance leads to more frequent maintenance, repairs, and part replacements. Consequently, maintenance-related downtime increases significantly, adversely affecting both productivity and profitability. Enhancing the wear resistance of surfaces that are prone to wear—such as those of shafts, mills, and gears—is thus of critical importance [4]. Thermochemical surface treatment methods, including carburizing, nitriding, and their combinations, have been widely recognized for improving the wear resistance of steels. These treatments are designed to selectively harden the surface layer of the material, thereby enhancing its durability without compromising the toughness of the core [5].

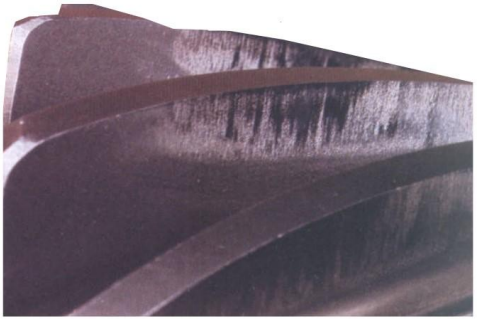

(a)

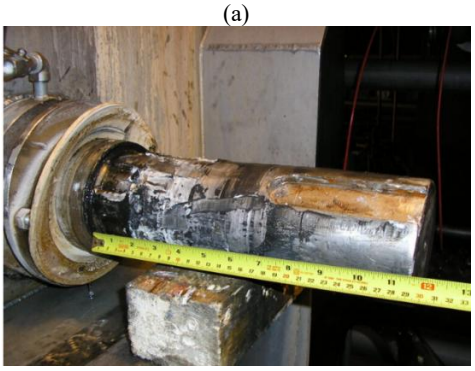

(b)

Figure 1: Representative images of wear damage from industry (a) Gear and (b) Shaft [6,7]

Nitriding is a thermochemical surface treatment process employed to enhance the fatigue strength, wear resistance, and corrosion resistance of steel components [8,9]. Following nitriding, the treated surface typically exhibits increased hardness [10], improved wear resistance [11] and fatigue performance [12], and superior corrosion resistance [13]. Among the various nitriding techniques, the two-stage nitriding process is particularly preferred when a deeper diffusion layer is required to improve mechanical properties, while maintaining the compound (white) layer within a controlled thickness to avoid brittleness or spalling [14].

Gas nitriding is among the most widely utilized nitriding techniques. In this process, nitrogen diffuses into the steel surface from an ammonia-rich atmosphere at temperatures within the ferrite–carbide phase region [15]. Due to the limited solubility of nitrogen in ferrite, two distinct layers are formed on the steel surface: the outer compound layer (commonly referred to as the white layer) and the inner diffusion layer. The compound layer primarily consists of iron nitrides, with ε ($Fe_2N_{1+\gamma}$) and γ' (Fe_4N) being the most prevalent phases [16]. This layer appears white under microscopic examination, as it is resistant to most conventional etching reagents. Beneath this, the diffusion layer extends inward and is characterized by interstitial nitrogen atoms dissolved in the ferrite matrix, forming a solid solution. The mechanical properties of the nitrided material are largely governed by the diffusion layer, which contributes to enhanced hardness, strength, and wear resistance through atomic diffusion mechanisms. In contrast, the compound layer plays a crucial role in determining the tribological and electrochemical behavior of the surface, offering improved frictional performance and corrosion resistance [17-24].

34CrNiAl7 steel, which contains the main alloying elements of aluminum (Al), chromium (Cr), and molybdenum (Mo), is classified as a nitriding steel according to international standards. Due to its excellent surface hardenability and mechanical strength, it is widely utilized in the manufacturing of machine components, particularly gears and shafts [25–26]. Among its alloying constituents, aluminum plays a key role in enhancing the nitriding response and overall performance. Through nitriding, the steel achieves superior wear, corrosion, and fatigue resistance, making it highly suitable for demanding engineering applications, especially in the production of machine elements [27]. The influence of nitriding conditions on the microstructure, mechanical properties, and wear behavior of 34CrNiAl7 steel has been extensively studied and well-documented in the literature. [26,28,31]. Altinsoy et al. [26, 28] investigated the nitriding behavior of 34CrAlNi7 steel under both single-stage and double-stage gas nitriding processes. Their research revealed that single-stage nitriding may result in a more uniform compound layer but limited diffusion depth, while double-stage nitriding can improve nitrogen penetration and promote the formation of beneficial nitride phases due to the controlled thermal and chemical gradients. 42CrMo4 steel, called reclamation steel, is classified as a low-alloy chromium-molybdenum grade. It exhibits moderate hardenability and offers superior strength and toughness compared to other steels within the same category. Due to its cost-effectiveness and favorable mechanical properties, 42CrMo4 is widely employed in industrial machinery components such as shafts, gears, and mills, typically in a heat-treated condition [23]. However, its performance can vary significantly depending on the operating environment. Components made from 42CrMo4 steel are prone to damage under severe working conditions, often necessitating frequent maintenance. Although this steel is predominantly employed in its heat-treated state, the presence of chromium and molybdenum significantly enhances its response to nitriding treatments, thereby improving surface characteristics such as hardness, wear resistance, and fatigue performance [24,29]. Mohamed Ali Terres et al. [29] investigated the influence of gas nitriding duration on the wear behavior of 42CrMo4 steel at 525 °C. Their findings revealed that extended nitriding times enhance the formation and stability of the compound and diffusion layers, leading to improved wear resistance. However, the nature of wear mechanisms is highly dependent on the test duration and surface condition.

In this study, the gas nitriding behavior and wear characteristics of 42CrMo4 steel were investigated to identify a more cost-effective alternative to 34CrNiAl7 steel, which is conventionally recognized as a nitriding-grade steel due to its Ni and Al content. Both steel specimens were subjected to double-step gas nitriding under identical process parameters, with the nitriding potential (Kn) in the furnace set to 3.2, consistent with the treatment conditions applied to 34CrNiAl7 steel. The microstructural and mechanical characteristics of the nitrided layers formed on the surfaces were analyzed, and their wear behavior under dry sliding conditions was thoroughly examined. The performance differences between the two materials, both subjected to identical nitriding conditions, were systematically compared through detailed analysis. This study offers a comprehensive evaluation of the influence of gas nitriding on the wear resistance of both steels, providing a comparative analysis of their wear resistance mechanisms.

2. Materials and Methods

2.1 Materials

42CrMo4 and 34CrNiAl7 steels used in the experimental studies were supplied by Sağlam Metal Industry Trade Inc. The chemical compositions of 42CrMo4 and 34CrNiAl7 steels are presented in Table 1.

Table 1. Chemical composition of 42CrMo4 and 34CrNiAl7 steels.

Steels	C	Cr	Mo	Ni	Al	Mn	Si	V	S	P
42CrMo4	0.42	1.10	0.25	0,040	0,038	0.76	0,26	0,010	0,019	0,016
34CrNiAl7	0.34	1.70	0.20	1.00	1.00	0,62	0,30	0,014	0,025	0,024

2.2 Heat Treatment of Materials

The schematic representation of the heat treatment stages applied to the steels before nitriding is shown in Figure 1. Initially, the steel samples preheated at a temperature of 200°C for 0,5 h were heated to 850 °C and held for 1 hour, followed by rapid quenching in oil to achieve the desired hardening effect. Upon completion of the cooling process, a two-step tempering treatment was performed to enhance the mechanical strength of the materials. This involved holding the specimens at 450 °C for 2 hours during each tempering cycle.

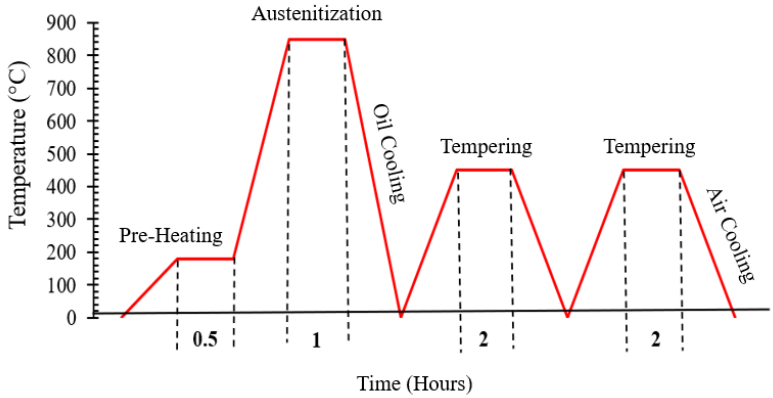

Figure 2. The schematic graph of the quenching+tempering heat treatment process applied to the 42CrMo4 and 34CrNiAl7 steels.

Gas nitriding was performed using a Nitrex-brand gas nitriding furnace located at Sağlam Metal Industry Trade Inc. The furnace atmosphere consisted of an oxygen-free, nitrogen-rich environment generated through a controlled mixture of nitrogen, ammonia, and dissociated ammonia. The system operated under a Kn value, controlled regime, utilizing advanced software that enables fully automated process control by continuously regulating the furnace conditions throughout the nitriding treatment. The Nitrex software uses the Kn value as an input parameter and automatically calculates and adjusts the nitriding potential via a hydrogen sensor integrated with a dual-loop controller. This setup ensures precise control over the nitriding process, contributing to consistent and reproducible surface treatment results [30].

The Lehrer diagram was originally developed by Lehrer to illustrate the relationship between temperature and nitriding potential for pure iron during nitriding processes. Constructed based on the equilibrium conditions of the NH_3–H_2 and Fe–N systems, the diagram serves as a valuable tool for estimating the nitride phases formed and the nitrogen concentration at a given temperature and nitriding potential. An extended version of the Lehrer diagram, incorporating additional isoconcentration lines, is presented in Figure 3. In this extended diagram, iron nitrides or solid solutions are shown in equilibrium with a specific nitriding atmosphere at a given temperature, as characterized by the (Kn). Although Lehrer diagrams have been adapted for certain alloy steels, the original diagram for pure iron remains useful for approximating the nitriding potential required to achieve desired surface properties in gas nitriding treatments. Accordingly, in this study, the initial nitriding potential was determined using the Lehrer diagram for pure iron [31–32]. A single (Kn) value was employed to achieve the formation of both a compound (white) layer and a diffusion layer. A Kn value of 3.2 and a process temperature of 575°C were selected based on the Lehrer diagram presented in Figure 3.

During the nitriding process, elevated temperatures can promote the formation of nitride networks along grain boundaries, particularly at sharp corners commonly found in industrial component designs. Such nitride networks may lead to localized damage and corner breakage. Therefore, the nitriding temperature was carefully chosen as 575 °C, corresponding to the selected Kn value of 3.2, due to its tendency to promote the formation of the ε-phase. According to the Lehrer diagram (Figure 3), the phase formation at 575 °C varies with nitriding potential: the α-Fe phase is expected for $Kn < 0.2$, the γ′ phase (Fe_4N, diffusion layer) for $0.3 < Kn < 1$, and the ε phase ($Fe_2(N,C)_{1-z}$, compound layer) for $Kn > 1.5$. At the intersection of 575 °C and $Kn = 3.2$, the nitrogen content in the ε-phase formed on the surface of both steels was estimated to be approximately 8.75%, based on the Lehrer diagram for pure iron.

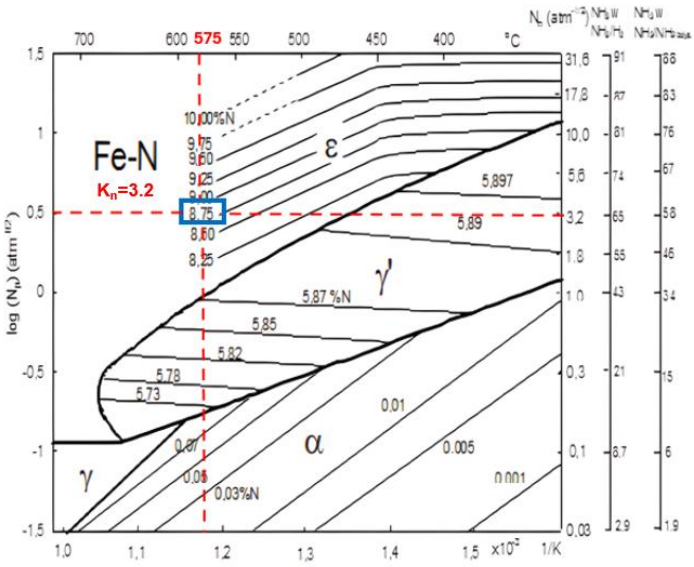

Figure 3. Extended Lehrer diagram with additional isoconcentration lines. In the diagram, iron nitride or solid solution is in equilibrium with a given nitriding atmosphere at a certain temperature [31].

In this study, a double-stage gas nitriding process was employed to achieve a deep diffusion layer while maintaining a controlled white layer thickness, as shown in Figure 4. Initially, the samples were heated from room temperature to 400°C. The first nitriding stage was conducted at elevated nitriding potentials (Kn) and low temperatures for 2 hours. This combination of high Kn and low temperature was selected to enhance the nitriding potential of the atmosphere, reduce the nucleation time of the white layer, and promote uniformity across the nitrided surface. As the first stage approached completion, the ammonia flow rate was increased by introducing 100% NH_3 into the system to stabilize the Kn value for the subsequent stage. Upon reaching thermal equilibrium, the samples were further heated to 575°C for the second nitriding stage. During this phase, the Kn value was maintained at 3.2% by supplying ammonia separately into the atmosphere. The second stage, characterized by a lower Kn and higher temperature, facilitated the desired surface nitrogen concentration while controlling the growth of the white layer. The gas nitriding process at 575°C was sustained for 3.5 hours, after which the samples were cooled using nitrogen gas. The temperature and duration of the treatment were determined based on the Lehrer diagram presented in Figure 3. It is important to note that the elevated temperatures used in the second stage may lead to the formation of nitride networks along grain boundaries, particularly at sharp corners in industrial component designs. These nitride networks can compromise structural integrity, resulting in corner damage, breakage, and spalling.

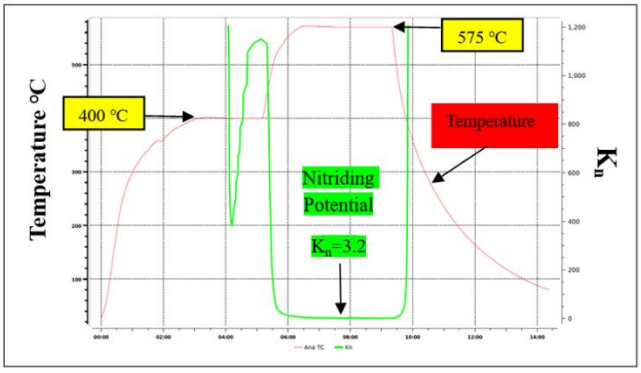

Figure 4. Gas nitriding process graph of 42CrMo4 and 34CrNiAl7 steels in gas nitriding Nitrex furnace system.

2.3 Microstructural Examination

For metallographic analysis, the surfaces and cross-sections of annealed, oil-quenched, and gas-nitrided 42CrMo4 and 34CrNiAl7 steel samples were prepared. The specimens were first wrapped in aluminum foil and mounted in bakelite. Grinding was performed sequentially using silicon carbide papers with grit sizes ranging from 240 to 2400. Subsequently, the samples were polished using

3 µm and 1 µm diamond suspensions to achieve a mirror-like finish. Chemical etching was carried out by immersing the polished samples in a 3% Nital solution (prepared by mixing 100 ml of distilled water with 3% HNO_3) for 5 seconds. Microstructural characterization of the etched samples was performed using a Nikon LV150N upright metallurgical microscope.

2.4 Hardness Measurements

Surface hardness measurements of the nitrided samples were performed using a Zwick Roell ZHV10 microhardness tester under a 200 g load (HV 0.2 Vickers microhardness test). Additionally, the nitriding hardness depth of the steels was characterized following the DIN 50190-3 standard [33]. According to this standard, the diffusion depth is defined as the distance from the surface to the point where the hardness value exceeds either 50 HV above the core hardness or 10% of the core hardness. Hardness profiles were obtained by performing measurements at 50 µm intervals along a line extending from the surface to the core on the cross-section of metallographically prepared samples. To ensure measurement reliability and statistical accuracy, three individual indentations were made at each depth point, and the average value was recorded.

2.5 Wear Test

Friction and wear tests of the gas-nitrided samples were conducted using a CSM-brand tribometer equipped with a Linear Reciprocating Test Module, following the ASTM G133 standard. The tests were performed under dry sliding conditions at applied loads of 10 N and 15 N, with a total sliding distance of 1000 m and a sliding speed of 0.30 m/s at room temperature. An Al_2O_3 ball was used as the counter material. The selected test loads enabled a direct comparison of the wear performance of both steels under identical laboratory conditions. Additionally, a load increment of 5 N was applied to assess whether the wear rate exhibited a linear response to increasing load. During testing, wear penetration depth and coefficient of friction (COF) data were continuously recorded by the tribometer. Each sample was weighed before and after testing using a precision balance with an accuracy of 0.0001 g, and the corresponding mass losses were documented. The wear rates of the gas-nitrided 42CrMo4 and 34CrNiAl7 steels were calculated based on the measured weight loss data. The specific wear rates were determined using Equation 2, as shown below [34]:

$$SWR = \Delta w / pxLxD \quad (1)$$

where the Δw is the measured weight loss (before and after the test), ρ is the density of the materials, which is the same for all samples (7.85-7.80 g/cm^3), L is the applied load (10-15N), and D is the sliding distance (1000m).

3. Results

The Fe-N binary phase diagram, which illustrates the equilibrium interaction between iron and nitrogen, can be utilized to estimate the phases likely to form during the gas nitriding process [35]. As depicted in the metastable Fe-N equilibrium diagram (Figure 5), the ε (epsilon) and γ′ (gamma prime) phases are nitrogen-rich compounds that typically form in the nitrided layer during treatment. Compared to the Fe-C phase diagram, the transformation temperatures in the Fe-N system are lower, allowing nitriding to be performed at reduced temperatures. This characteristic presents a significant advantage of nitriding over other thermochemical treatments such as carburizing and boriding. The two principal phases in the Fe-N system, as shown in Figure 5, are $Fe_4N_{1+\gamma}$ (commonly referred to as the γ′ phase) and Fe_2N_{1-x} (known as the ε phase), both of which contribute to the formation of the white layer during gas nitriding. When the nitrogen concentration exceeds the solubility limit in α-Fe (ferrite), the γ′ phase is the first to form on the surface, typically at nitrogen contents between 5.7 and 6.1 wt%. The γ′-$Fe_4N_{1+\gamma}$ phase possesses a stable structure in which nitrogen atoms occupy the interstitial sites of the face-centered cubic lattice formed by iron atoms [36]. At temperatures above 680°C, γ′ transforms into the ε-$Fe_{2-3}N$ phase. This ε phase, which exists within the compound layer, is a solid solution based on Fe_3N and is represented as ε-$Fe_{2-3}N$. In this structure, nitrogen atoms occupy the interstitial positions within a densely packed hexagonal lattice of iron atoms. The ε phase is ferromagnetic, and its eutectoid decomposition into γ and γ′ phases occurs at approximately 650°C [37]. The fundamental metallurgical mechanisms underlying the gas nitriding process—a thermochemical surface treatment—are governed by the phase transformations described in the Fe-N phase diagram.

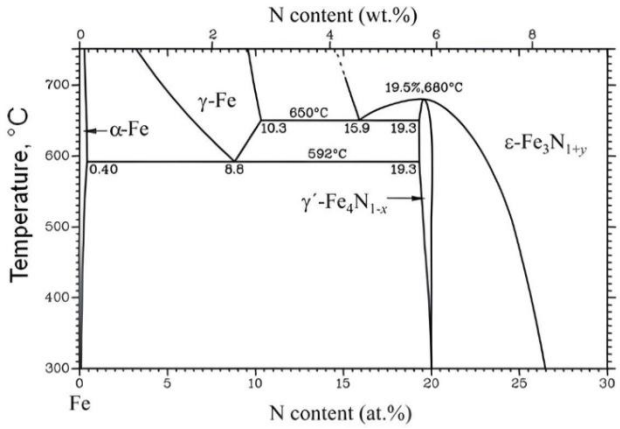

Figure 5. Fe-N Binary diagram [38].

During gas nitriding conducted below the eutectoid temperature (590 °C for the pure iron–nitrogen system), under conditions where ε-$Fe_2(N,C)_{1-x}$ is thermodynamically stable, the gear material intended for industrial applications undergoes specific thermochemical transformations, as illustrated in Figure 6. This figure also depicts the formation of the compound (white) layer and the diffusion zone resulting from the nitriding process, as observed in the microstructure. As shown in Figure 6, when the process is carried out below the eutectoid temperature, ammonia gas undergoes thermal dissociation upon contact with the heated metal surface. This reaction can be represented as follows:

$$2NH_3 \rightarrow N_2 + 3H_2 \quad (2)$$

The atomic nitrogen generated through this dissociation diffuses into the metal substrate, initiating the formation of nitride phases such as γ′-Fe_4N and ε-$Fe_{2-3}N$, depending on the local nitrogen concentration and temperature. These phases contribute to the development of the compound layer, which enhances surface hardness and wear resistance.

The gas nitriding process is endothermic, meaning it absorbs thermal energy from the surrounding environment. The metal surface acts as a catalyst, facilitating the decomposition of ammonia (NH_3) and enabling the release of atomic nitrogen (N). Due to its high diffusion coefficient, atomic nitrogen readily penetrates the metal substrate, establishing a concentration gradient between the nitrogen-rich surface and the nitrogen-deficient interior. This gradient drives the diffusion of nitrogen atoms inward, governed by the difference in chemical potential. As nitrogen migrates into the steel matrix, it reacts with alloying elements to form nitride compounds. In steels, typical nitride phases include various forms of iron nitrides, such as ε-$Fe_{2-3}N$ and γ'-Fe_4N. The formation and distribution of these nitride phases are crucial to the surface hardening effect achieved through gas nitriding. The specific phases formed, as well as their morphology and depth, are influenced by the steel's chemical composition and the nitriding temperature [15].

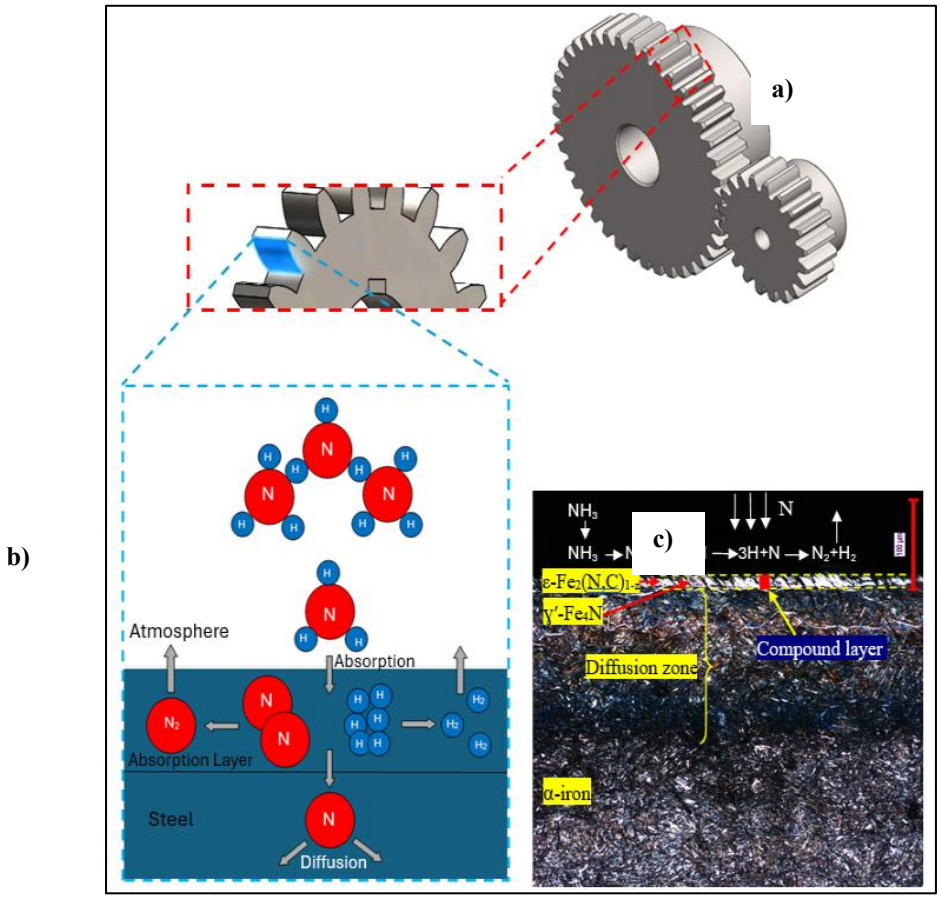

Figure 6. a) Gear material intended for industrial use, b) Schematic representation of the chemical reactions occurring during the gas nitriding process, c) Cross-sectional microstructure of the surface layer formed on the gear material after gas nitriding treatment

3.1 Microstructural Investigations

The annealed microstructures of 42CrMo4 and 34CrNiAl7 steels are presented in Figure 7 (a, c), while the microstructures following oil quenching and tempering—applied as a hardening heat treatment—are shown in Figure 7 (b, d). The annealed 42CrMo4 steel, containing 0.42 wt.% carbon, exhibits a dual-phase microstructure composed of ferrite and pearlite, with both fine and coarse morphologies, indicative of a coarse-grained structure. The observed variation in morphological dimensions is attributed to an irregular cooling gradient during the annealing process. As shown in Figure 7 (b), the microstructure of quenched and tempered (Q+T) 42CrMo4 steel reveals a transformation of the ferrite and pearlite phases into martensite, along with the presence of retained austenite. These observations are consistent with the findings of Linton Carvajal et al. [39], who reported that annealed 42CrMo4 steel consists of ferrite and pearlite, whereas the Q+T condition results in a tempered martensitic structure. Similarly, the annealed microstructure of 34CrNiAl7 steel (Figure 7c) displays ferrite and pearlite phases, while the Q+T microstructure (Figure 7d) is characterized by tempered martensite.

As depicted in Figure 7 (a–d), retained austenite is evident in the microstructures of both steels following oil quenching and tempering. The 34CrNiAl7 steel, in particular, exhibits a greater proportion of retained austenite compared to 42CrMo4. This increased retention is attributed to the presence of 1 wt.% Nickel in the chemical composition of 34CrNiAl7, as outlined in Table 1. Nickel is known to lower the martensite start (Ms) temperature, thereby reducing the driving force for martensitic transformation during cooling. As a result, a slower cooling rate is required to achieve a martensitic structure comparable to that of nickel-free steels such as 42CrMo4. These findings are consistent with the observations reported in [40]

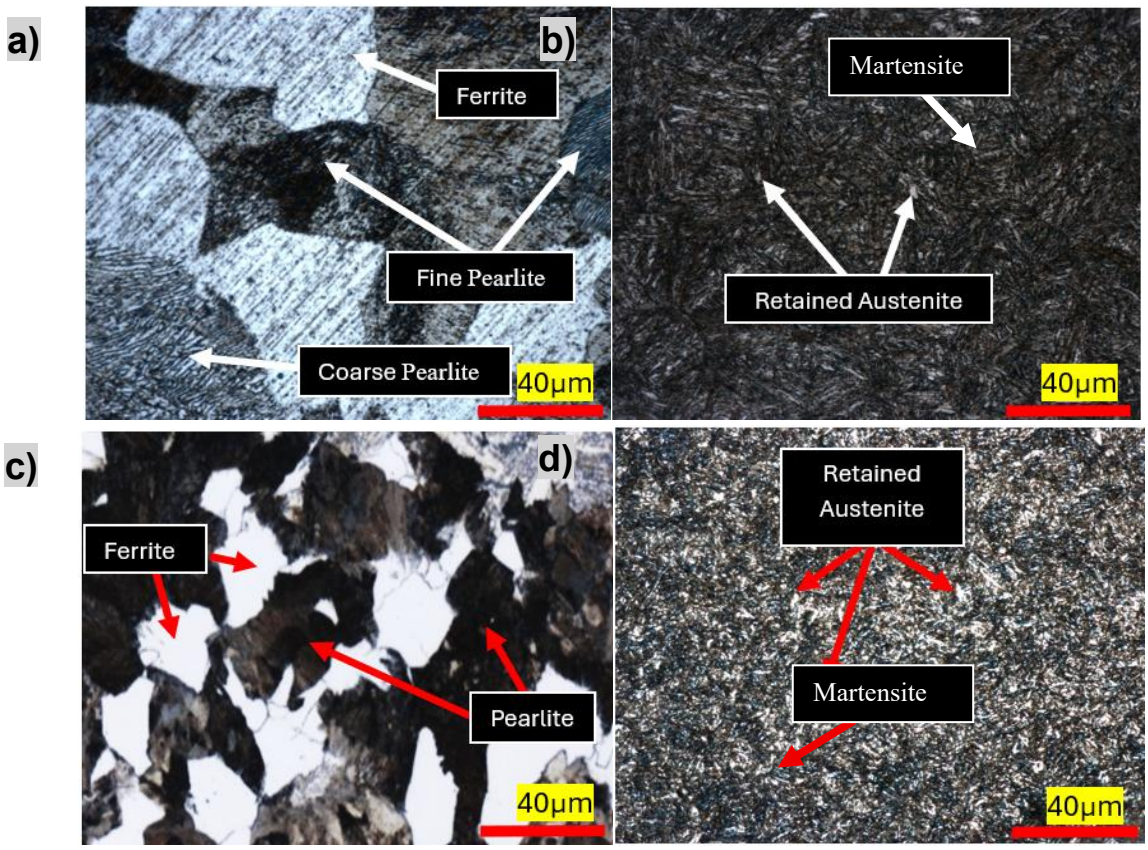

Figure 7. Microstructure images of 42CrMo4 and 34CrNiAl7 steel. (a) Annealed 42CrMo4 steel, (b) Oil-quenched and tempered 42CrMo4 steel, (c) Annealed 34CrNiAl7 steel, (d) Oil-quenched and tempered 34CrNiAl7 steel.

Cross-sectional micrographs of gas-nitrided 42CrMo4 and 34CrNiAl7 steels are presented in Figure 8. Both materials exhibit a continuous and uniform white layer at the surface, indicative of a well-developed compound zone. This layer, predominantly composed of iron nitrides, demonstrates a dense and coherent structure, with no observable porosity. The average thickness of the compound layer was measured to be 17.11 µm for 42CrMo4 steel and 12.33 µm for 34CrNiAl7 steel, respectively

Optical microscopy of the diffusion zones beneath the compound layers in gas-nitrided 42CrMo4 and 34CrNiAl7 steels revealed distinct microstructural differences between the two materials. In contrast to 42CrMo4, the diffusion zone in 34CrNiAl7 steel was more clearly discernible in the optical micrographs of the nitrided region. This zone reflects a gradual nitrogen concentration gradient and the formation of nitrides with alloying elements. The enhanced visibility of the diffusion zone in 34CrNiAl7 steel is likely attributable to its aluminum content (1 wt.%), a potent nitride-forming element. Aluminum exhibits a strong affinity for nitrogen, resulting in the formation of stable aluminum nitrides [34]. This behavior is believed to contribute to the development of a thinner and more compact compound layer, as well as a more pronounced diffusion zone. Furthermore, aluminum in the alloy promotes the formation of the γ′ phase in the form of $(Fe,Al)_4N$ by enhancing intergranular nitrogen diffusion. The γ′ phase preferentially grows along grain boundaries and slip planes, often manifesting as whisker-like structures [41–43].

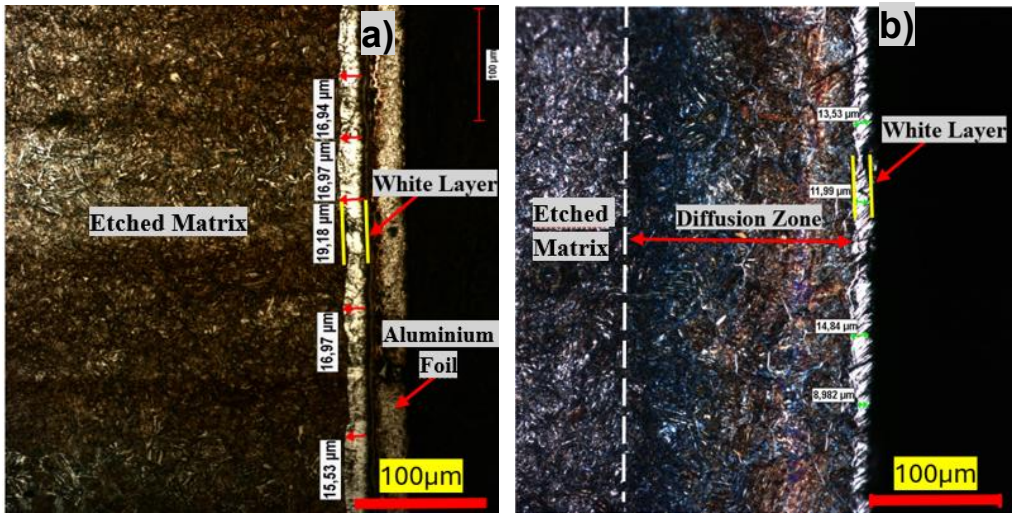

Figure 8. Microstructure images of gas nitrided (a) 42CrMo4 and (b) 34CrNiAl7 steel from the cross-section at 200X.

3.2 Hardness Test Results

Figure 9 illustrates the surface hardness profiles of 42CrMo4 and 34CrNiAl7 steels following quenching+tempering, as well as subsequent gas nitriding. Post-quenching and tempering, the hardness values of 42CrMo4 and 34CrNiAl7 steels were recorded as 241 HV and 239 HV, respectively. A significant enhancement in surface hardness was observed in both materials after gas nitriding, while the core hardness remained largely unchanged. The surface hardness increased to 650 HV for 42CrMo4 and 1050 HV for 34CrNiAl7 following gas nitriding, indicating that 34CrNiAl7 achieved approximately 60% higher surface hardness. From core to surface, the hardness of 42CrMo4 increased by approximately 170%, whereas 34CrNiAl7 exhibited a 340% increase. This significant improvement in 34CrNiAl7 steel is attributed to its alloying composition, particularly the presence of aluminum, which promotes the formation of hard nitride phases and enhances surface strengthening. As one of the most potent nitride-forming elements, aluminum facilitates the formation of high-hardness aluminum nitride (AlN) compounds during gas nitriding [44]. This contributes to the development of a harder and more wear-resistant surface layer in 34CrNiAl7 steel compared to 42CrMo4. Supporting evidence from Dobrocký et al. indicates that gas nitriding of 42CrMo4 steel at 530 °C for 7 hours resulted in the formation of an 18.4 µm thick compound layer and a surface hardness of 637 HV 0.1.

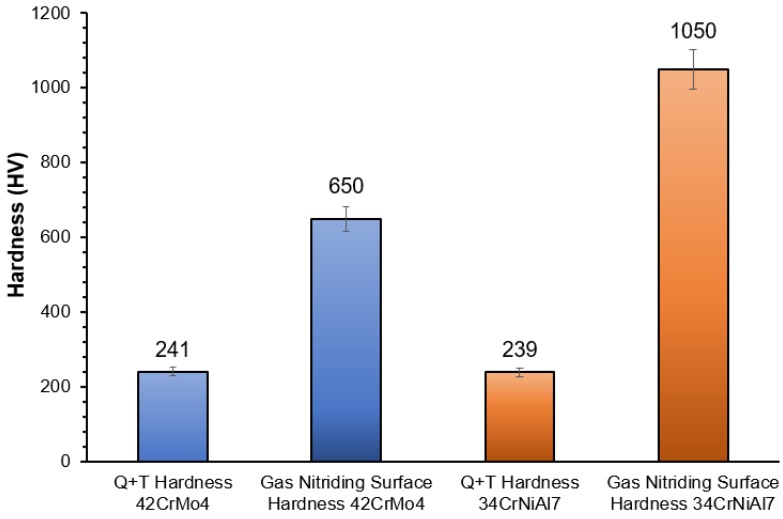

Figure 9. Surface hardnesses of 42CrMo4 and 34CrNiAl7 steels measured after quenching+tempering heat treatment and gas nitriding.

The effective case depth resulting from gas nitriding was evaluated by the DIN 50190-3 standard, based on hardness profiles obtained through gradual measurements from the core to the surface. These profiles offer a practical means of assessing nitrogen diffusion without the need for advanced chemical characterization techniques. The effective hardness depth was found to be greater in 42CrMo4 steel (approximately 317.6 µm) compared to 34CrNiAl7 steel (approximately 191.4 µm). The hardness gradient in 42CrMo4 steel exhibited a more gradual increase, which corresponded to a lower surface hardness. Although the diffusion zone was not distinctly visible in metallographic examinations, the hardness profile confirmed nitrogen diffusion into the substrate to a measurable extent. Additionally, the core hardness remained unchanged following nitriding, indicating that the core hardness of both steels post-treatment was equivalent to their initial core hardness prior to nitriding.

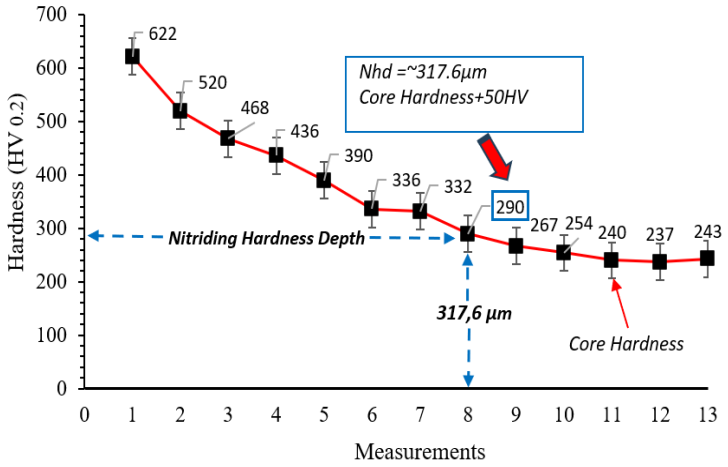

Figure 10. Effective hardness depth profile of the gas nitride 42CrMo4 steel.

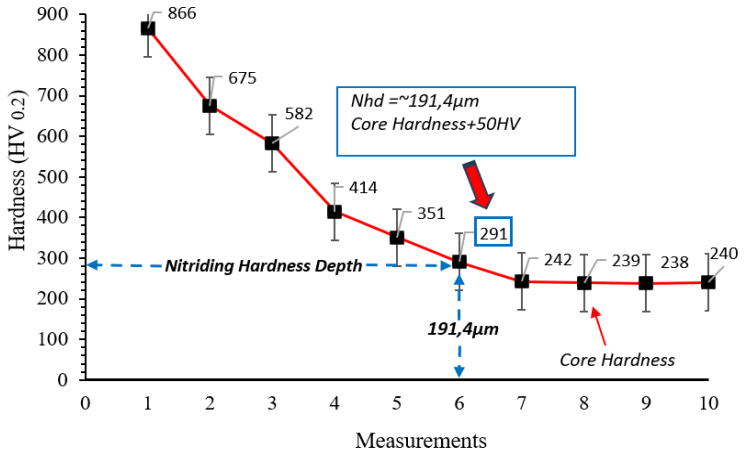

Figure 11. Effective hardness depth profile of the gas nitrided 34CrNiAl7 steel.

The properties of the gas-nitrided region are influenced not only by the process parameters but also by the type and concentration of alloying elements present in the steel. In the present study, both 42CrMo4 and 34CrNiAl7 steels were subjected to gas nitriding under identical processing conditions. Consequently, a comparative evaluation of their nitriding behavior based on compositional differences offers valuable insights. While 42CrMo4 primarily contains chromium (Cr) and molybdenum (Mo) as its main alloying elements, 34CrNiAl7 incorporates additional elements such as nickel (Ni) and aluminum (Al), resulting in a higher overall alloying content. Figures 12(a) and 12(b) illustrate the influence of alloying elements and their respective concentrations on surface hardness and nitriding depth. An increase in alloying content generally correlates with enhanced surface hardness following nitriding [44]. However, elevated alloy concentrations tend to impede the growth of the nitrided layer by reducing the nitrogen diffusion rate into the matrix. As depicted in Figure 12(a), Cr, Mo, and Al are identified as the most effective nitride-forming elements due to their strong affinity for nitrogen [44]. The substantial thermodynamic driving force for nitride precipitation facilitates the formation of a diffusion zone enriched with nano-sized nitrides dispersed within the ferrite matrix [35]. Among these elements, Al exerts the most pronounced effect on hardness, whereas Ni exhibits minimal influence on the hardness of the nitrided layer. Although the nucleation of hexagonal AlN is thermodynamically favorable, it is hindered by a significant lattice mismatch with the ferrite matrix. As a result, AlN tends to precipitate in a metastable cubic (NaCl-type) structure, which preferentially nucleates on dislocations generated by γ′ phase precipitation. This cubic modification promotes the formation of a harder nitrided layer in Al-containing steels such as 34CrNiAl7 [36].

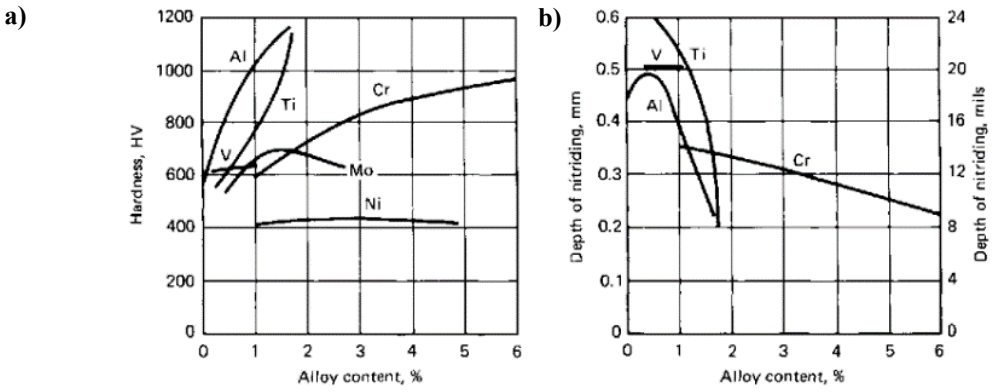

Figure 12. Effect of alloying element percentages on (a) hardness and (b) nitriding depth of steels after nitriding [45].

3.3 Wear Test Result

The tribological performance of gas-nitrided 42CrMo4 and 34CrNiAl7 steels was comparatively evaluated through dry sliding wear tests conducted under normal loads of 10 N and 15 N over a sliding distance of 1000 meters at room temperature. The assessment parameters included weight loss, wear penetration depth, wear rate, and coefficient of friction. The weight loss data are illustrated in Figure 13. Under a 10 N load, 42CrMo4 steel exhibited a weight loss of 0.031 g, which increased to 0.058 g under a 15 N load. In contrast, 34CrNiAl7 steel showed lower weight losses of 0.022 g and 0.037 g under the same respective loads. These results indicate that the weight loss of 42CrMo4 steel was approximately 40% higher at 10 N and 56% higher at 15 N compared to 34CrNiAl7 steel. These findings indicate that gas-nitrided 34CrNiAl7 steel demonstrates superior wear resistance under both low and high applied loads, with its performance being particularly more pronounced at higher load conditions. The enhanced tribological behavior of 34CrNiAl7 steel is attributed to its higher surface hardness and improved resistance to plastic deformation. The formation of γ′ and ε phases on the surface of 34CrNiAl7 steel during the gas nitriding process significantly contributed to its enhanced wear resistance. In particular, the ε phase, which is promoted by the presence of aluminum and nitrogen, resulted in a harder surface layer than that of 42CrMo4 steel (see Figure 9), thereby reducing wear-induced material loss [46].

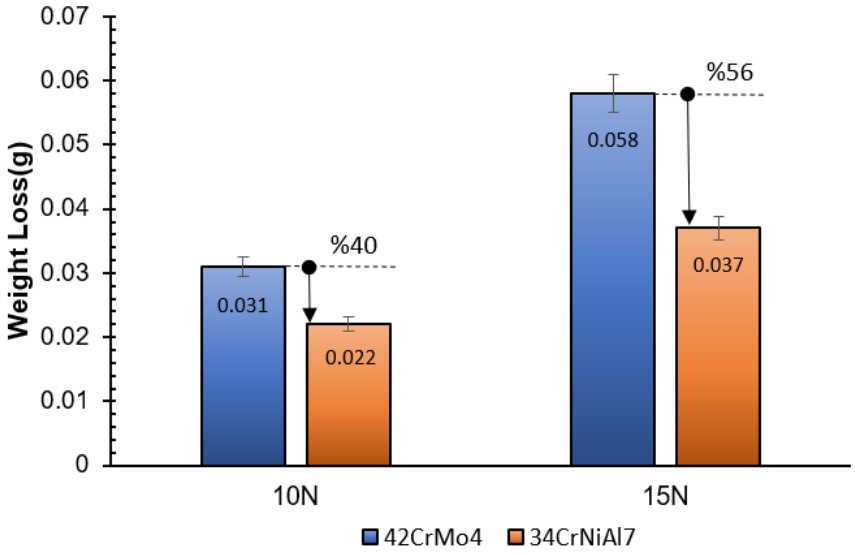

Figure 13. Weight loss of gas nitrided 42CrMo4 and 34CrNiAl7 steels after wear test under 10 and 15 N load.

Figure 14 presents the wear penetration depth profiles of gas-nitrided 42CrMo4 and 34CrNiAl7 steels following dry sliding wear tests conducted under normal loads of 10 N and 15 N. Under a 10 N load, the penetration depth of 42CrMo4 steel was measured at 0.0564 µm, whereas 34CrNiAl7 steel exhibited a lower depth of 0.0357 µm. Similarly, under a 15 N load, the wear depth increased to 0.0755 µm for 42CrMo4 steel and 0.0469 µm for 34CrNiAl7 steel. These results indicate that 42CrMo4 steel experienced deeper wear penetration under both loading conditions, reflecting its comparatively lower wear resistance. The consistency between the wear track depth and weight loss results further reinforces the superior tribological performance of 34CrNiAl7 steel.

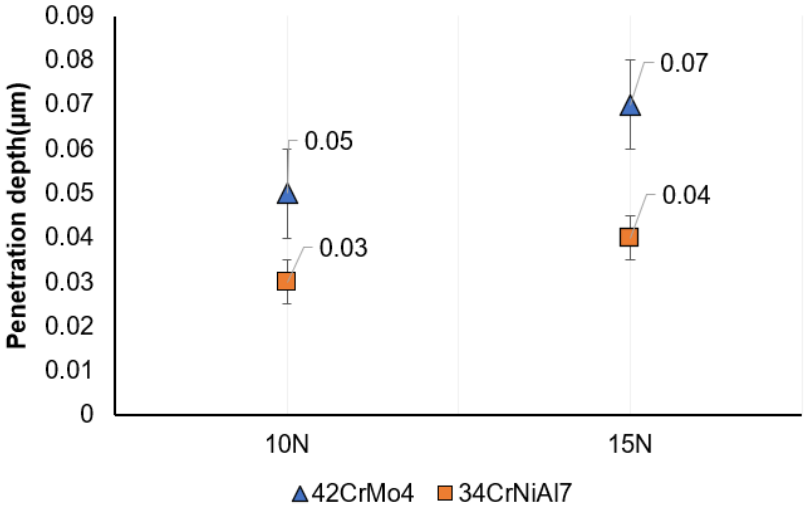

Figure 14. Wear penetration depths of gas nitrided 42CrMo4 and 34CrNiAl7 steels after wear test under 10 and 15 N load.

Figure 15 illustrates the wear rates of gas-nitrided 42CrMo4 and 34CrNiAl7 steels, calculated using Equation (1) based on the weight loss data obtained from dry sliding wear tests. The wear rate of both steels increased with the application of higher loads. This increase is attributed to the expansion of the contact area between the abrasive Al_2O_3 ball and the nitrided steel surface under elevated loads, which intensifies the wear process by concentrating stress over a smaller surface area. Consequently, this leads to more severe material removal per unit sliding distance. Specifically, the wear rate of gas-nitrided 42CrMo4 steel increased by 24%, while that of 34CrNiAl7 steel increased by 12% when the load was raised from 10 N to 15 N. The greater sensitivity of 42CrMo4 steel to increased load highlights its comparatively lower wear resistance. The superior performance of 34CrNiAl7 steel is attributed to the formation of a harder nitride white layer on its surface during the nitriding process. Notably, the surface hardness of 34CrNiAl7 steel is approximately 400 HV higher than that of 42CrMo4 steel, which enhances its resistance to plastic deformation mechanisms such as sliding and grooving, thereby reducing wear-induced material loss [47].

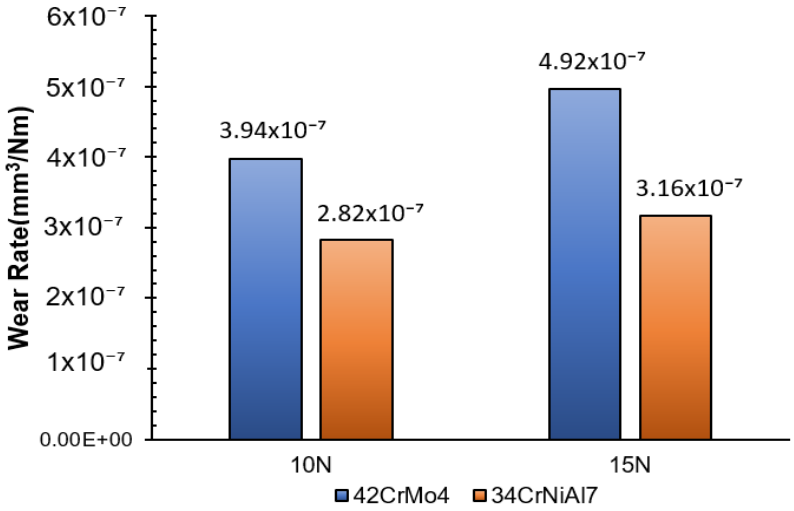

Figure 15. Wear rates calculated from the weight losses of gas nitrided 42CrMo4 and 34CrNiAl7 steels after the wear test under 10 and 15 N loads.

Figure 16 presents the average friction coefficients calculated during dry sliding wear tests conducted under applied loads of 10 N and 15 N for gas-nitrided 42CrMo4 and 34CrNiAl7 steels. Under both loading conditions, 34CrNiAl7 steel exhibited lower friction coefficients compared to 42CrMo4 steel. This reduction in friction is attributed to the formation of the $(Fe,Al)_4N$ compound during the gas nitriding process, which occurs in the presence of aluminum and is known to yield lower friction values. In contrast, 42CrMo4 steel primarily forms the Fe_4N compound. Previous studies have investigated the frictional behavior of these compounds within the white layer [48–49], reporting friction coefficients of approximately 0.3 for AlN and 0.5 for FeN, respectively. The presence of AlN in the nitrided layer of 34CrNiAl7 steel is therefore considered a key factor contributing to its lower friction coefficient. Additionally, the whisker-like nitride networks observed in the cross-sectional microstructure of 34CrNiAl7 steel are believed to enhance the adhesion of the nitrided layer to the substrate, thereby preventing micro-cracking and delamination. This microstructural feature contributes to a smoother contact surface, further supporting the reduced friction behavior observed in the 34CrNiAl7 alloy.

On the other hand, a thicker white layer was observed on the surface of 42CrMo4 steel compared to 34CrNiAl7 steel. Panfil-Pryka et al. [50] applied a gas nitriding process to 42CrMo4 steel at 570 °C for 5 hours and reported the formation of an ε-phase layer, with an average white layer thickness of 24.7 µm. They performed dry sliding wear tests at various temperatures. At room temperature, a friction coefficient of 0.73 was recorded for an average white layer thickness of 24.7 µm. Similarly, Dobrocký et al. [51] reported that gas nitriding of 42CrMo4 steel at 530 °C for 7 hours resulted in a white layer thickness of 18.4 µm and a surface hardness of 637 HV0.1. The observed difference in white layer thickness may be attributed to furnace inhomogeneity or uncontrolled adjustment of the nitriding potential (Kn value). Under high contact stresses, a thicker white layer may become more brittle, increasing the likelihood of microcracks or surface fractures. Literature reports indicate that such surface damage can elevate friction by generating wear debris and disrupting smooth contact conditions [52–53].

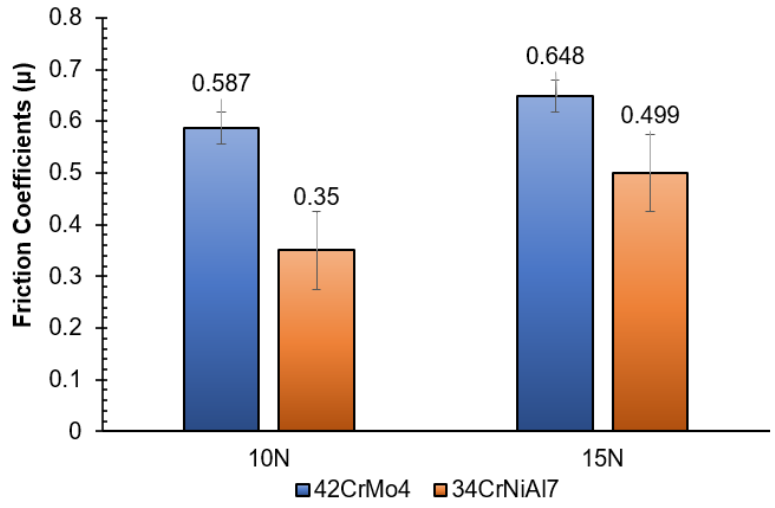

Figure 16. Average friction coefficients of gas nitrided 42CrMo4 and 34CrNiAl7 steels wear tested under 10 and 15N loads.

4. Conclusions

This study presents a comparative evaluation of the microstructural, mechanical, and tribological properties of gas-nitrided 42CrMo4 and 34CrNiAl7 steels. The key findings are summarized as follows:

- Following oil quenching and tempering heat treatment, both steel specimens exhibited tempered martensitic microstructures. The resulting hardness values were found to be nearly identical, indicating comparable mechanical performance under the applied thermal conditions. However, 34CrNiAl7 steel retained more austenite due to its higher nickel content.
- The surface hardness of 42CrMo4 steel increased from 241 HV to 650 HV, representing a 169% improvement. In contrast, 34CrNiAl7 steel exhibited a more substantial enhancement, with hardness rising from 239 HV to 1050 HV—a 339% increase. These results highlight the significant influence of alloy composition on the effectiveness of the nitriding process.

- The double-stage gas nitriding process led to the formation of compound (white) layers with average thicknesses of 17.11 µm in 42CrMo4 steel and 12.33 µm in 34CrNiAl7 steel. These results indicate a material-dependent response to the nitriding treatment, likely influenced by differences in alloy composition and diffusion kinetics.

- Diffusion depths were measured as 317.6 µm for 42CrMo4 steel and 191.4 µm for 34CrNiAl7 steel, indicating a deeper nitrogen penetration in the former. This disparity may be attributed to differences in alloy composition, microstructural characteristics, and diffusion kinetics, which influence the nitriding response of each material.

- Wear tests demonstrated that 42CrMo4 steel exhibited higher wear rates and friction coefficients under both applied loads (10 and 15 N), suggesting inferior tribological performance compared to 34CrNiAl7 steel. This behavior may be attributed to differences in surface hardness, microstructural characteristics, and the effectiveness of the nitrided layer in resisting wear.

- The superior wear resistance of 34CrNiAl7 steel was attributed to the formation of a harder nitride layer, comprising γ′ (gamma prime) and ε (epsilon) phases. This phase development was facilitated by the presence of aluminum and nickel in the alloy, which promotes the formation and stability of these hard nitrides during the nitriding process.

From an industrial standpoint, the selection of nitrided steel should be guided by the severity of wear conditions. For components subjected to high mechanical stress and severe wear—such as aerospace landing gear, high-load gears, and metal forming tools—gas-nitrided 34CrNiAl7 steel is recommended due to its superior surface hardness and wear resistance. Conversely, for applications involving moderate wear, such as hydraulic rods, camshafts, and general-purpose industrial shafts, gas-nitrided 42CrMo4 steel offers a cost-effective and sufficiently durable alternative, balancing toughness and wear resistance.

Author Contributions

5. References

[1] Gorka-Kostrubiec, B. (2015). The magnetic properties of indoor dust fractions as markers of air pollution inside buildings. *Building and Environment*, *90*, 186-195.

[2] Prof.Dr. Yüksel.M. ‘’ Malzeme Bilgisi ‘’ Makine Mühendisleri Odası, İstanbul, 2002.

[3] Wulpi, Donald J. "Failures of shafts." (2002).

[4] Neale, M., & Gee, M. (2001). *A guide to wear problems and testing for industry*. William Andrew.

[5] Czerwinski, F. (2012). Thermochemical treatment of metals. *Heat Treatment–Conventional and Novel Applications*, *5*, 73-112.

[6] Belzona, ‘wear damage of shafts and gears’ (https://blog.belzona.com/worn-shaft-repair/)

[7] Errichello, R., & Muller, J. (2002). How to analyze gear failures. *Journal of Failure Analysis and Prevention*, *2*(6),8-16.

[8] T. Sun, T. Bell (1991). Mater. Sci. Eng., 140, 419–434.

[9] Yang, Mei. (2012). Nitriding--Fundamentals, Modeling and Process Optimization. Diss. Worcester Polytechnic Institute.

[10] Alekseeva, M. S., Gress, M. A., Scherbakov, S. P., Gerasimov, S. A., & Kuksenova, L. I. (2017). The influence of high-pressure gas nitriding on the properties of martensitic steels. *Metal Science and Heat Treatment*, *59*, 524-528.

[11] Singh, S. K., Naveen, C., Sai, Y. V., Satish, U., Bandhavi, C., & Subbiah, R. (2019). Experimental study on wear resistance of AISI 347 treated with salt bath nitriding and gas nitriding processes-a review. *Materials Today: Proceedings*, *18*, 2717-2722.

[12] Kim, Y. H., & Kim, H. G. (2010). Effect of Gas Nitriding Characteristics on the Mechanical Properties after Pre-Heat Treatment of Stainless Steels. *Journal of the Korean Society for Heat Treatment*, *23*(3), 142-149.

[13] Michalski, J., Wach, P., Tacikowski, J., Betiuk, M., Burdynski, K., Kowalski, S., & Nakonieczny, A. (2009). Contemporary industrial application of nitriding and its modifications. *Materials and Manufacturing Processes*, *24*(7-8), 855-858.

[14] Nam, Nguyen Duong ve diğerleri. "Kontrol gazı nitrürleme işlemi: Bir inceleme." *J. Mekanik. Çayır. Karar. Gelişme* 42.1 (2019): 17-25.

[15] Pye, D. (2003). *Practical nitriding and ferritic nitrocarburizing*. ASM international.

[16] Mohammadzadeh, R., Akbari, A., & Drouet, M. (2014). Microstructure and wear properties of AISI M2 tool steel on RF plasma nitriding at different N2–H2 gas compositions. *Surface and Coatings Technology*, *258*, 566-573.

[17] Wang, C. J., & Jaw, J. H. (2004). Study of wear behavior of nitride layers in Fe–Mn–Al–C alloys. *Surface and Coatings Technology*, *177*, 477-482.

[18] Baranowska, J., Franklin, S. E., & Pelletier, C. G. N. (2005). Tribological behaviour and mechanical properties of low temperature gas nitrided austenitic steel in relation to layer morphology. *Wear*, *259*(1-6), 432-438.

[19] Manova, D., Hirsch, D., Richter, E., Mändl, S., Neumann, H., & Rauschenbach, B. (2007). Microstructure of nitrogen implanted stainless steel after wear experiment. *Surface and Coatings Technology*, *201*(19-20), 8329-8333.

[20] Marchev, K., Cooper, C. V., & Giessen, B. C. (1998). Observation of a compound layer with very low friction coefficient in ion-nitrided martensitic 410 stainless steel. *Surface and Coatings Technology*, *99*(3), 229-233.

[21] Xia, Y., Wang, S., Zhou, F., Wang, H., Lin, Y., & Xu, T. (2006). Tribological properties of plasma nitrided stainless steel against SAE52100 steel under ionic liquid lubrication condition. *Tribology international*, *39*(7), 635-640.

[22] Terres, M. (2003, January). Fatigue behaviour of an ion nitrided steel. In *Annales de Chimie, Science des Materiaux* (Vol. 28, No. 1, pp. 25-41).

[23] Baranowska, J., Franklin, S. E., & Kochmańska, A. (2007). Wear behaviour of low-temperature gas nitrided austenitic stainless steel in a corrosive liquid environment. *Wear*, *263*(1-6), 669-673.

[24] Kesti, E. (2009). Ç-4140 çeliğinin, mikro yapı ve mekanik özelliklerine su verme ortamının etkilerinin araştırılması.

[25] Ginter, C., Torchane, L., Dulcy, J., Gantois, M., Malchère, A., Esnouf, C., & Turpin, T. (2006). A new approach to hardening mechanisms in the diffusion layer of gas nitrided? -alloyed steels. Effects of chromium and aluminium: experimental and simulation studies. *La metallurgia italiana*.

[26] Altinsoy, I., Çelebı Efe, G., Yener, T., Önder, K., & Bindal, C. (2017). Effect of double stage nitriding on 34CrAlNi7-10 nitriding steel. *Acta Physica Polonica A*, *132*(3), 663-666.

[27] Lugscheider, E., Bobzin, K., & Lackner, K. (2003). Investigations of mechanical and tribological properties of CrAlN+ C thin coatings deposited on cutting tools. *Surface and Coatings Technology*, *174*, 681-686.

[28] Altinsoy, I., Onder, K., Celebi Efe, F., & Bindal, C. (2014). Gas nitriding behaviour of 34CrAlNi7 nitriding steel. *Acta Physica Polonica A*, *125*(2), 414-416.

[29] Terres, M. A., Ammari, L., & Chérif, A. (2017). Study of the effect of gas nitriding time on microstructure and wear resistance of 42CrMo4 steel. *Materials Sciences and Applications*, *8*(06), 493.

[30] Bell, T. (1991). Gaseous and plasma nitrocarburizing. *ASM International, ASM Handbook.*, *4*, 425-436.

[31] Önder, K. G. (2013). *Gaz nitrürlemede işlem parametrelerinin 34CrAlNi7 çeliğinin mekanik özelliklerine etkisi* (Master's thesis, Sakarya Universitesi (Turkey)).

[32] Atmani, H., & Thoumire, O. (2002). Microstructure characterization of fluidized bed nitrided Fe-Si and Fe-Si-Al foils. *Bulletin of Materials Science*, *25*, 219-225.

[33] DIN 50190-3 – Hardness depth of heat-treated parts; determination of the effective depth of hardening after nitriding. Deutsches Institut für Normung E. V., 1979.

[34] Singla, I., Kumar, H., Pahlevani, F., Handoko, W., Cholake, S. T., Hossain, R., & Sahajwalla, V. (2019). From waste to surface modification of aluminum bronze using selective surface diffusion process. *Scientific Reports*, *9*(1), 1559.

[35] Du, H., & Hillert, M. (1991). An Assessment of the Fe-CN System/Überarbeitung des Systems Fe-CN. *International Journal of Materials Research*, *82*(4), 310-316.

[36] Lee, B. J. (2006). A modified embedded-atom method interatomic potential for the Fe–C system. *Acta materialia*, *54*(3), 701-711.

[37] Meka, S. R. (2011). Nitriding of iron-based binary and ternary alloys: microstructural development during nitride precipitation.

[38] ASM Handbook. Vol. 3. Alloy phase diagrams. ASM International. Handbook Commitee. Materials Park; Ohio: ASM International. 1992.

[39] Carvajal, L., Artigas, A., Monsalve, A., & Arévalo, E. (2017). Monitoring heat treatments in steels by a non-destructive ultrasonic method. *Materials Research*, *20*(Suppl 2), 347-352.

[40] Yu, Q., Zhao, Y., & Zhao, F. (2024). Influence of Nickel on Microstructure and Mechanical Properties in Medium-Carbon Spring Steel. *Materials*, *17*(10), 2423.

[41] Lakhtin, Y. (1996). Metal Sci. Heat Treatm. 38, 6.

[42] Korwin, M., Liliental, W., Maldzinski, L., Czelusniak, A., & Tymowski, G. (1999). Nitreg controlled gas Nitriding an enviroment-friendly process for surface hardening of steel. *Nitrex Metal Inc., Canada*.

[43] Lakhtin, Y. M., Silina, N. V., & Fedchun, V. A. (1981). Nature of the high hardness and brittleness of the nitrided case on steel 38Kh2MYuA. *Metal Science and Heat Treatment*, *23*(3), 162-165.

[44] Bindumadhavan, P. N., Makesh, S., Gowrishankar, N., Wah, H. K., & Prabhakar, O. (2000). Aluminizing and subsequent nitriding of plain carbon low alloy steels for piston ring applications. *Surface and Coatings Technology*, *127*(2-3), 251-258.

[45] Schneider, M. J., & Chatterjee, M. S. (2013). Introduction to surface hardening of steels. In *Steel Heat Treating Fundamentals and Processes* (pp. 389-398). ASM International.

[46] Terres, M. A., Ammari, L., & Chérif, A. (2017). Study of the effect of gas nitriding time on microstructure and wear resistance of 42CrMo4 steel. *Materials Sciences and Applications*, *8*(06), 493.

[47] Solis Romero, J., Medina Flores, A., Roblero Aguilar, O., & Oseguera Peña, J. (2013). Tribological evaluation of plasma nitride H13 steel. *Superficies y vacío*, *26*(4), 131-138.

[48] Gao, S., Li, H., Kang, R., Zhang, Y., & Dong, Z. (2021). Effect of strain rate on the deformation characteristic of AlN ceramics under scratching. *Micromachines*, *12*(1), 77.

[49] Tong, W. P., Sun, J., Zuo, L., He, J. C., & Lu, J. (2011). Study on wear and friction resistance of nanocrystalline Fe nitrided at low temperature. *Wear*, *271*(5-6), 653-657.

[50] Panfil-Pryka, D., Kulka, M., Kotkowiak, M., Michalski, J., & Grochalski, K. (2024). Tribological Behavior of Gas-Nitrided 42CrMo4 Steel at High Temperatures. Coatings, 15(1), 18.

[51] Dobrocký, D., Joska, Z., Procházka, J., Svoboda, E., & Dostál, P. (2021). Evaluation of structural and mechanical properties of the nitrided layer on steel for weapons. *Manufacturing Technology*, *21*(2), 184-192.

[52] Aghajani, H., & Behrangi, S. (2017). *Plasma nitriding of steels* (pp. 1-67). Cham, Switzerland: Springer International Publishing.

[53] Wang, B., Zhao, X., Li, W., Qin, M., & Gu, J. (2018). Effect of nitrided-layer microstructure control on wear behavior of AISI H13 hot work die steel. *Applied Surface Science*, *431*, 39-43.